

Communications in Computational Physics

<http://journals.cambridge.org/CPH>

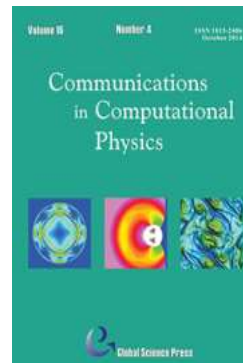
Additional services for *Communications in Computational Physics*:

Email alerts: [Click here](#)

Subscriptions: [Click here](#)

Commercial reprints: [Click here](#)

Terms of use : [Click here](#)



A Discontinuous Galerkin Method for Pricing American Options Under the Constant Elasticity of Variance Model

David P. Nicholls and Andrew Sward

Communications in Computational Physics / Volume 17 / Issue 03 / March 2015, pp 761 - 778
DOI: 10.4208/cicp.190513.131114a, Published online: 24 March 2015

Link to this article: http://journals.cambridge.org/abstract_S1815240615000171

How to cite this article:

David P. Nicholls and Andrew Sward (2015). A Discontinuous Galerkin Method for Pricing American Options Under the Constant Elasticity of Variance Model. *Communications in Computational Physics*, 17, pp 761-778 doi:10.4208/cicp.190513.131114a

Request Permissions : [Click here](#)

A Discontinuous Galerkin Method for Pricing American Options Under the Constant Elasticity of Variance Model

David P. Nicholls* and Andrew Sward

Department of Mathematics, Statistics, and Computer Science, University of Illinois at Chicago, Chicago, IL 60607, USA.

Received 19 May 2013; Accepted (in revised version) 13 November 2014

Communicated by Jan S. Hesthaven

Abstract. The pricing of option contracts is one of the classical problems in Mathematical Finance. While useful exact solution formulas exist for simple contracts, typically numerical simulations are mandated due to the fact that standard features, such as early-exercise, preclude the existence of such solutions. In this paper we consider derivatives which generalize the classical Black-Scholes setting by not only admitting the early-exercise feature, but also considering assets which evolve by the Constant Elasticity of Variance (CEV) process (which includes the Geometric Brownian Motion of Black-Scholes as a special case). In this paper we investigate a Discontinuous Galerkin method for valuing European and American options on assets evolving under the CEV process which has a number of advantages over existing approaches including adaptability, accuracy, and ease of parallelization.

AMS subject classifications: 91G20, 91G60, 65M70

Key words: Option pricing, PDE methods, CEV process, Discontinuous Galerkin method.

1 Introduction

The pricing of option contracts is one of the classical problems in Mathematical Finance [11, 14, 20]. While useful exact solution formulas exist for simple contracts (e.g., vanilla European calls/puts) [11, 14, 20], typically numerical simulations are mandated due to the fact that standard features, such as early-exercise (e.g., an American contract), preclude the existence of such solutions. We point out the work of Zhu [23] which explicitly describes a solution procedure for American options, however, the method is both quite

*Corresponding author. *Email addresses:* davidn@uic.edu (D. P. Nicholls), swardandphi@gmail.com (A. Sward)

complicated and very slowly converging. In this paper we consider derivatives which generalize the classical Black-Scholes setting by not only admitting the American feature, but also considering assets which evolve by the Constant Elasticity of Variance (CEV) process (which includes the Geometric Brownian Motion-GBM-of Black-Scholes as a special case) [2, 6, 12, 22]. We consider American options not only for their intrinsic interest, but also because they are more common than Europeans [11]. We consider the CEV model as this is one of the most popular methods for capturing the “volatility smile” implied by option prices in the financial markets [22].

While there are myriad techniques for numerically simulating such options, they typically fall into one of three categories: Binomial methods, Monte Carlo methods, and PDE methods [11, 14, 20]. Binomial methods are both quite flexible (American features can be accommodated nearly seamlessly) and simple to implement, but have a rather slow (errors like $1/M$ in M , the number of nodes [11]) and non-monotonic convergence. The interested reader is referred to the illustrative computations in Chapter 16 of [11] for representative simulations, and for a concrete implementation (which we utilize later in this paper) we refer the reader to Lu & Hsu [17]. The Monte Carlo method is also extremely flexible (particularly for contracts with complex features or those based upon multiple assets) and relatively straightforward to code. These approaches are more difficult to extend to American contracts and suffer from *extremely* slow rates of convergence (errors proportional to $1/\sqrt{M}$ for M samples [11]) which necessitates sophisticated “variance reduction” techniques [11, 14] to generate competitive algorithms. We point out that Glasserman [10] provides a Monte Carlo method for the CEV process. Additionally, we refer the reader to the work of Hsu, Lin, & Lee [12], Lo, Tang, Ku, & Hui [18], and Knessl & Xu [16] for further results on pricing options on assets evolving under the CEV process.

PDE methods have their own list of advantages and shortcomings which render them the method of choice for pricing options under certain sets of conditions [11, 14, 20]. PDE methods solve the Black-Scholes PDE (or its generalization) *directly* which leads to the value of the option for *all* possible asset prices and times between inception and expiry of the contract. While this certainly is more information than is typically required, it does mean that sensitivity information from the Greeks can be approximated with little or no extra cost. Additionally, as PDE methods admit the possibility of *high-order* simulation for Europeans (i.e., featuring errors which decay like C/M^p , integer $p \geq 1$, or even $Ce^{-\kappa M}$, $\kappa > 0$, for M unknowns), the number of degrees of freedom required to deliver an option price with a fixed tolerance may be comparable to (or smaller than) that required by binomial or Monte Carlo simulation.

In this paper we investigate a PDE method for valuing both European and American options on assets evolving under the CEV process which has a number of advantages over existing approaches including adaptability, arbitrary-order accuracy (for Europeans), and ease of parallelization. Approaches to valuing options based upon Finite Difference (FDMs) and Finite Element Methods (FEMs) are, by now, classical [11, 14, 20] and typically couple either second-order central differencing to implicit time stepping (resulting in the Crank-Nicolson method), or piecewise-linear basis functions to implicit time

stepping (in the FEM context). For Europeans both are second-order in space and time discretization (errors proportional to $1/M^2$ where M is the number of spatial/temporal gridpoints) and unconditionally stable. Furthermore, in this context both can be generalized to higher order (errors proportional to $1/M^p$) in exchange for an increase in computational cost and difficulty of implementation (wider difference stencils for FDMs, higher-order basis functions for FEMs, and multiple intermediate time steps). In this way both FDMs and FEMs accommodate hp -refinement (where $h \sim 1/M$ is the grid-spacing) which indicates that more accurate solutions can be realized by reducing h and/or increasing p . We refer the interested reader to the encyclopedic text of Achdou & Pironneau [1] for further details and extensions (see also [5] for more recent results). An important point to make is that arbitrary-order accuracy for *any* PDE approach for American options is problematic as, at the early-exercise boundary, the solution is only guaranteed to have continuity in the first derivative. This fact will limit the spatial accuracy of any scheme (typically only first order) [21] unless special treatments are designed (see, e.g., the refinement strategies of Willyard [21]) which we do not pursue here.

Despite all of this, these PDE methods are still limited (even for Europeans) in a number of ways. First, FDMs require equally-spaced grids which precludes the possibility of adapted spatial meshes that would allow clustering of gridpoints near points of interest (e.g., near the strike price). FEMs, on the other hand allow general meshes (elements may be arbitrarily sized), however, the inter-element continuity requirement results in a *global* constraint on the problem unknowns which can make efficient implementations (particularly on parallel architectures) very challenging.

Since the late 1990's there has been a surge of interest in FEMs which do *not* require continuity across element boundaries (see [15] for a complete history). At first glance this appears to complicate the scheme as not only will there be more degrees of freedom to resolve, but also decisions need to be made at element boundaries to determine these unknowns. However, it was quickly realized that this additional freedom can be used to enforce desirable properties in the resulting Discontinuous Galerkin (DG) methods. Of particular note, in the case of hyperbolic PDEs (e.g., wave equations, systems of hyperbolic conservation laws), the element boundary conditions (encoded via "numerical fluxes") could be specified to be "upwinding" to deliver stability to these schemes. An additional benefit of this approach is the localization that this approach enjoys: Information at element boundaries must still be exchanged, however, it is now done rather "weakly" through the numerical flux rather than "strongly" via enforced continuity. As a result of this, implementations on massively parallel architectures are quite easy to imagine and we see this as a particular strength of our approach [15]. While this is not necessary for pricing options on a single asset as considered here, it is mandated for options on baskets of assets, for instance, which certainly fit into the context of the work presented here. We point the interested reader to the recent work of Vos, Sherwin, and Kirby [19] concerning parallelization and performance of spectral/ hp element methods.

We are aware of only one other description of DG methods applied to options pricing problems [13]. In this a DG method is outlined for pricing vanilla European calls/puts in

the standard Black-Scholes framework of GBM. Our work extends that of [13] to American options under the CEV process. We mention also the work of Foufas & Larson [9] which describes a DG method in the time variable.

The organization of the paper is as follows: In Section 2 we review the differential equations and final/boundary conditions which govern the value of options on assets following the CEV process. In Section 2.1 we recall exact solutions, in Section 2.2 we review the details of the model in the case of the CEV process, and in Section 2.3 we point out special considerations which must be made for American options. In Section 3 we describe our Discontinuous Galerkin approach to pricing American options in the CEV model, with specifics for our Generalized Black-Scholes PDE presented in Section 3.1 and the American feature and time stepping in Section 3.2. Finally, in Section 4 we present numerical results which display the accuracy and reliability of our algorithms.

2 Governing equations

In this paper we consider options based upon an asset which follows the Constant Elasticity of Variance (CEV) process [2, 6, 22]. In this case the asset price $S = S(t)$ satisfies the Stochastic Differential Equation

$$dS = \mu S dt + \sigma S^\alpha dW, \quad (2.1)$$

where μ is the “drift,” σ is the “volatility,” α is the “elasticity,” and W is a Wiener process. We point out that for $\alpha = 1$ we recover the classical Geometric Brownian Motion (GBM), for $\alpha = 1/2$ we realize the square-root model, while $\alpha = 0$ gives the Ornstein-Uhlenbeck process.

It is reported in Wong & Zhao [22] that since the financial crisis of 1987, the volatility smile used to price equity options increases as the stock price decreases, i.e. $\alpha < 1$. By contrast, for options on futures, the volatility increases as the stock price increases, i.e. $\alpha > 1$.

2.1 Exact solutions

Consider a European call or put struck at E expiring at $t = T$ based upon an asset following the CEV process (2.1). Exact solution formulas exist for the time-zero value of these options, more specifically, Cox [6] derived

$$C_E = S_0 \{1 - \chi^2(b, c + 2, d)\} - E e^{-rT} \chi^2(d, c, b), \quad (2.2a)$$

$$P_E = E e^{-rT} \{1 - \chi^2(d, c, b)\} - S_0 \chi^2(b, c + 2, d), \quad (2.2b)$$

when $\alpha < 1$, while Emanuel and MacBeth [8] show that

$$C_E = S_0 \{1 - \chi^2(d, -c, b)\} - E e^{-rT} \chi^2(b, 2 - c, d), \quad (2.3a)$$

$$P_E = E e^{-rT} \{1 - \chi^2(b, 2 - c, d)\} - S_0 \chi^2(d, -c, b), \quad (2.3b)$$

when $\alpha > 1$. In these

$$b = \frac{(Ee^{-rT})^{2(1-\alpha)}}{(1-\alpha)^2w}, \quad c = \frac{1}{1-\alpha}, \tag{2.4}$$

and

$$d = \frac{S^{2(1-\alpha)}}{(1-\alpha)^2w}, \quad w = \frac{\sigma^2}{2r(\alpha-1)} \left\{ e^{2r(\alpha-1)T} - 1 \right\}, \tag{2.5}$$

and $\chi^2(z, k, \ell)$ is the cumulative distribution function of a noncentral chi-squared random variable with noncentrality parameter ℓ and k degrees of freedom.

As reported in [22], subroutines to compute the function χ^2 are widely available, however, they are rather unstable and extremely expensive. We refer the interested reader to Figure 2.4 and Table 2.1 of [22], which display, respectively, the prohibitive cost and instability of numerical implementations of this function in the limiting case $\alpha \rightarrow 1$. Oddly, this “singular” value is where the simple Black-Scholes formula for GBM is valid! These computations vividly display in a quantitative and explicit manner that simply because a “closed-form” solution exists to a problem, it is not necessarily to one’s advantage to use it. Rather, [22] demonstrate that in this setting one should use a *numerical approximation* based upon numerical solution of the Generalized Black-Scholes PDE, (2.7), which is the approach we advocate in this contribution.

2.2 Generalized Black-Scholes and the PDE approach

It is a classical argument [11,14,20] to show that the fair price, $V = V(S, t)$, for a European option based upon an asset, $S = S(t)$, undergoing a GBM satisfies the Black-Scholes PDE

$$\partial_t V + \frac{\sigma^2}{2} S^2 \partial_S^2 V + rS \partial_S V - rV = 0, \quad S \geq 0, \quad 0 \leq t \leq T. \tag{2.6}$$

A straightforward generalization to the case of an asset following the CEV model (2.1) satisfies the “Generalized Black-Scholes” (GBS) PDE [22]

$$\partial_t V + \frac{\sigma^2}{2} S^{2\alpha} \partial_S^2 V + rS \partial_S V - rV = 0, \quad S \geq 0, \quad 0 \leq t \leq T. \tag{2.7}$$

This must be supplemented with a final condition $V(S, T) = V_T(S)$, which, for calls and puts struck at E , is

$$V_T^C(S) = \max\{S - E, 0\}, \quad V_T^P(S) = \max\{E - S, 0\}, \tag{2.8}$$

respectively, and boundary conditions. For a European call these are typically chosen to be [11,14,20]

$$C(0, t) = 0, \quad C(S, t) \sim S, \quad \text{as } S \rightarrow \infty, \tag{2.9}$$

and, for a European put,

$$P(0, t) = Ee^{-rt}, \quad P(S, t) \rightarrow 0, \quad \text{as } S \rightarrow \infty. \tag{2.10}$$

2.3 American options

The American feature in an option allows one to exercise at any time up to, and including, expiry. It is well-known [11,14,20] that this leads to a *moving-boundary* problem: One must not only solve a PDE, but also determine its domain of definition, which *moves* in time. For simple options a single “optimal exercise price,” $S = S^*(t)$ exists which separates the set of prices for which one should exercise early from those where you should not. Additionally, in the absence of dividend payments, this boundary does *not* exist for calls (Higham [11] displays explicitly that early-exercise is not optimal in this instance) and thus we focus on puts from here.

Let $P = P(S,t)$ be the value of an American put, struck at E and expiring at T , and $S = S^*(t)$ be the optimal exercise price. Then the entire domain is divided into two regions separated by the moving optimal exercise boundary: In the *exercise region*

$$\partial_t P + \frac{\sigma^2}{2} S^{2\alpha} \partial_S^2 P + rS \partial_S P - rP < 0, \quad 0 < S < S^*(t), \quad 0 < t < T, \quad (2.11a)$$

$$P(S,t) = E - S = \max\{E - S, 0\}, \quad (2.11b)$$

while in the *continuation region*

$$\partial_t P + \frac{\sigma^2}{2} S^{2\alpha} \partial_S^2 P + rS \partial_S P - rP = 0, \quad S > S^*(t), \quad 0 < t < T, \quad (2.12a)$$

$$P(S,t) > \max\{E - S, 0\}. \quad (2.12b)$$

On the free boundary, we enforce continuity of the option value and its first S partial derivative (the “delta”)

$$P(S^*(t), t) = E - S^*(t), \quad \partial_S P(S^*(t), t) = -1; \quad (2.13)$$

the latter condition is the “smooth pasting condition” [11, 14, 20].

3 A Discontinuous Galerkin method

To specify the Discontinuous Galerkin (DG) method for pricing European and American put options under the CEV process, we begin by introducing some notation. For full details we refer the interested reader to the authoritative text of Hesthaven & Warburton [15]. Denote the problem domain and boundary, respectively, by

$$\Omega = [0, S_{\max}], \quad \partial\Omega = \{0, S_{\max}\}. \quad (3.1)$$

We subdivide the domain into K nonoverlapping elements, D^k , so that

$$\Omega = \bigcup_k D^k. \quad (3.2)$$

The local inner product and $L^2(D^k)$ norm are:

$$\langle u, v \rangle_{D^k} := \int_{D^k} uv dx, \quad \|u\|_{D^k}^2 := \langle u, u \rangle_{D^k}. \quad (3.3)$$

For this one-dimensional case, $D^k = [x_l^k, x_r^k]$, and on each element we represent the solution as a polynomial of order $N = N_p - 1$:

$$u_h^k(x, t) := \sum_{n=1}^{N_p} \hat{u}_n^k(t) \psi_n(x) = \sum_{i=1}^{N_p} u_h^k(x_i^k, t) \ell_i^k(x), \quad x \in D^k, \quad (3.4)$$

where the first is known as the modal form (the ψ_n are a local polynomial basis) and the second is known as the nodal form (where the ℓ_i are the interpolating Lagrange polynomials),

$$\ell_i(x) := \prod_{j=1, j \neq i}^{N_p} \frac{x - x_j}{x_i - x_j}, \quad \ell_i(x_j) = \delta_{i,j}. \quad (3.5)$$

Proceeding as in Hesthaven & Warburton [15] we map our intervals to a reference element:

$$x(r) = x_l^k + \left(\frac{1+r}{2}\right) h^k, \quad h^k = x_r^k - x_l^k, \quad r \in [-1, 1], \quad (3.6)$$

for $x \in D^k$. We can now choose our basis and gridpoints on the reference element and map them to the physical grid.

At this point we specify the modal basis functions, and for this we select

$$\psi_n(r) = \tilde{P}_{n-1}(r) = \frac{P_{n-1}(r)}{\sqrt{\gamma_{n-1}}}, \quad (3.7)$$

where $P_n(r)$ are the Legendre polynomials of order n and $\gamma_n = 2/(2n+1)$. For the modes, \hat{u}_n , we assume our modal representation is interpolatory:

$$u(r_i) = \sum_{n=1}^{N_p} \hat{u}_n \tilde{P}_{n-1}(r_i), \quad (3.8)$$

for the gridpoints r_i . In matrix form we have:

$$\mathcal{V} \hat{\mathbf{u}} = \mathbf{u}, \quad (3.9)$$

where

$$\mathcal{V}_{i,n} = \tilde{P}_{n-1}(r_i), \quad \hat{\mathbf{u}}_{\mathbf{n}} = \hat{u}_n, \quad \mathbf{u}_{\mathbf{i}} = u(r_i), \quad (3.10)$$

and \mathcal{V} is a generalized Vandermonde matrix.

Evidently, the choice of gridpoints will define the Vandermonde matrix and determine its conditioning. A case can be made [15] for the N_p zeros of:

$$f(r) = (1-r^2) \tilde{P}'_N(r). \quad (3.11)$$

These are known as the Legendre-Gauss-Lobatto (LGL) quadrature points, and the local (nodal) mass matrix on the reference element is now given by:

$$\mathcal{M}_{i,j} = \langle \ell_i, \ell_j \rangle_{[-1,1]} = (\mathcal{V}\mathcal{V}^T)_{i,j}^{-1}. \quad (3.12)$$

Transforming back to the element D^k we have:

$$\mathcal{M}_{i,j}^k = \frac{h^k}{2} \mathcal{M}_{i,j}, \quad (3.13)$$

and the local (nodal) stiffness matrix on the reference element is given by:

$$\mathcal{S}_{i,j} = \langle \ell_i, \ell'_j \rangle_{[-1,1]} = \langle \ell_i, \ell'_i \rangle_{D^k} = \mathcal{S}_{i,j}^k. \quad (3.14)$$

If we define

$$\mathcal{D}_{r,(i,j)} = \ell'_j \Big|_{r_i}, \quad (3.15)$$

then

$$\mathcal{M}\mathcal{D}_r = \mathcal{S}, \quad \mathcal{D}_r = \mathcal{V}_r \mathcal{V}^{-1}, \quad (3.16)$$

where

$$\mathcal{V}_{r,(i,j)} = \tilde{P}'_j \Big|_{r_i}. \quad (3.17)$$

3.1 The generalized Black-Scholes PDE

To describe the specific details of our DG scheme as applied to our GBS model (2.7), we first reverse time,

$$\tau = T - t, \quad (3.18)$$

and then rewrite it as

$$\partial_\tau V = \partial_S \left(\frac{\sigma^2}{2} S^\alpha S^\alpha \partial_S V \right) + \left(rS^{1-\alpha} - \sigma^2 \alpha S^{\alpha-1} \right) S^\alpha \partial_S V - rV. \quad (3.19)$$

Following the developments of [15], we write this as a system of two first-order PDEs, by setting $q = S^\alpha \partial_S V$ giving

$$\partial_\tau V = \partial_S \left(\frac{\sigma^2}{2} S^\alpha q \right) + \left(rS^{1-\alpha} - \sigma^2 \alpha S^{\alpha-1} \right) q - rV, \quad (3.20a)$$

$$q = S^\alpha \partial_S V. \quad (3.20b)$$

Turning to our numerical method, we approximate

$$\begin{pmatrix} V(S,t) \\ q(S,t) \end{pmatrix} \approx \begin{pmatrix} V_h(S,t) \\ q_h(S,t) \end{pmatrix} = \bigoplus_{k=1}^K \begin{pmatrix} V_h^k(S,t) \\ q_h^k(S,t) \end{pmatrix} = \bigoplus_{k=1}^K \sum_{i=1}^{N_p} \begin{pmatrix} V_h^k(S_i,t) \\ q_h^k(S_i,t) \end{pmatrix} \ell_i^k(S), \quad (3.21)$$

where \oplus is the direct sum. Thus we are representing V and q by $(N_p - 1)$ -th order piecewise polynomials on K elements. We form the residuals for the GBS equation:

$$R_h^k(S, t) = \partial_\tau V_h^k - \partial_S \left(\frac{\sigma^2}{2} S^\alpha q_h^k \right) - \left(rS^{1-\alpha} - \sigma^2 \alpha S^{\alpha-1} \right) q_h^k + rV_h^k, \quad (3.22a)$$

$$Q_h^k(S, t) = q_h^k - S^\alpha \partial_S V_h^k, \quad (3.22b)$$

and require that the residuals are orthogonal to our nodal basis functions represented as the interpolating Lagrange polynomials $\ell_i^k(S)$:

$$\int_{D^k} R_h^k \ell_i^k dS = 0, \quad \int_{D^k} Q_h^k \ell_i^k dS = 0, \quad 1 \leq i \leq N_p. \quad (3.23)$$

Integration by parts yields:

$$\begin{aligned} & \int_{D^k} \left(\partial_\tau V_h^k - \left(rS^{1-\alpha} - \sigma^2 \alpha S^{\alpha-1} \right) q_h^k + rV_h^k \right) \ell_i^k dS + \int_{D^k} \frac{\sigma^2}{2} S^\alpha q_h^k (\ell_i^k)' dS \\ &= \int_{\partial D^k} \hat{\mathbf{n}} \cdot \frac{\sigma^2}{2} S^\alpha q_h^k \ell_i^k dS, \end{aligned} \quad (3.24)$$

and

$$\int_{D^k} \left(q_h^k - S^\alpha \partial_S V_h^k \right) \ell_i^k dS = 0. \quad (3.25)$$

Substitution of the nodal forms yields:

$$\mathbf{M}^k \left(\partial_\tau \mathbf{V}_h^k - \mathbf{A} \mathbf{q}_h^k + r \mathbf{V}_h^k \right) = -\mathbf{S}^T \left(\frac{\sigma^2}{2} \mathbf{q}_h^k \right) + \int_{\partial D^k} \hat{\mathbf{n}} \cdot \frac{\sigma^2}{2} \left(S^\alpha \mathbf{q}_h^k \right)^* \ell^k dS, \quad (3.26)$$

where $(\cdot)^*$ denotes the “numerical flux,” and the second equation, $q = S^\alpha \partial_S V$, yields

$$\mathbf{M}^k \mathbf{q}_h^k = -\tilde{\mathbf{S}}^T \mathbf{V}_h^k + \int_{\partial D^k} \hat{\mathbf{n}} \cdot (S^\alpha \mathbf{V}_h^k)^* \ell^k dS. \quad (3.27)$$

In these

$$\mathbf{M}_{i,j}^k = \langle \ell_i^k, \ell_j^k \rangle, \quad \mathbf{S}_{i,j} = \langle S^\alpha \ell_i^k, (\ell_j^k)' \rangle, \quad \tilde{\mathbf{S}}_{i,j} = \langle \ell_i^k, (S^\alpha \ell_j^k)' \rangle, \quad \mathbf{A}_{i,j} = rS_{i,j}^{1-\alpha} - \sigma^2 \alpha S_{i,j}^{\alpha-1}. \quad (3.28)$$

As we mentioned in the Introduction, treatment of inter-element jumps is accomplished by the “numerical flux.” With this one can mandate physically relevant behavior from our DG scheme, for instance, “upwinding” for hyperbolic problems. In our case, as the governing equations are essentially parabolic (e.g., the heat equation), there is natural dissipation and no preferred direction of propagation, we submit to conventional wisdom and, setting $u_h := (V_h, q_h)$, appeal to a central flux [15]

$$u_h^* = \{ \{ u_h \} \} := \frac{u^- + u^+}{2}, \quad (3.29)$$

where u^- is the limiting value of u from the *interior*, while u^+ is the limiting value of u from the *exterior*.

Remark 3.1. In both the computation of \mathbf{S} and $\tilde{\mathbf{S}}$, and the integral involving \mathbf{A} , we make the computationally advantageous “commutation approximation” discussed in Hesthaven & Warburton [15, pp. 253–254] where the powers S , e.g. S^α , are moved *outside* their inner products (integrals) and simply evaluated at the GLL points $S_{i,j}$. In this way only the standard differentiation matrix is required and “this simplification does not appear to impact the accuracy of the method substantially.” [15, p. 254].

Remark 3.2. In all of our simulations the semi-infinite domain $0 < S < \infty$ is truncated for numerical simulation to the domain $0 < S < S_{\max}$ as done in [22, see Equations (2.8) & (2.9)].

3.2 The American feature and time stepping

Regarding the American feature which we intend to simulate, we appeal to the classical approach of Brennan & Schwartz [4,20] who recast the problem as a Linear Complementarity Problem (LCP) of the form

$$\mathcal{A}\mathcal{B} = 0, \quad \mathcal{A} \geq 0, \quad \mathcal{B} \geq 0, \quad (3.30)$$

where $\mathcal{A} = \mathcal{A}(u_h, q_h)$ is specified by the pair of equations, (3.26) & (3.27), rearranged to have zero on the right-hand-side, and

$$\mathcal{B} = \mathcal{B}(u_h, q_h) = (u_h - \Lambda(S), q_h - S^\alpha \partial_S \Lambda(S))^T, \quad (3.31)$$

where $\Lambda(S) = \max\{E - S\}$ is the payoff at expiry.

For time-stepping we use the standard fourth-order explicit Runge-Kutta method [3]. Despite the CFL condition which must be respected, explicit time-stepping makes American option valuation easy when formulated as an LCP [4,20]. We simply enforce at each time step that the value of the option satisfies

$$V_{i,j} = \max\{V_{i,j}, \Lambda(S_{i,j})\}, \quad (3.32)$$

which also allows us to keep track of the moving boundary.

4 Numerical results

We now demonstrate the capabilities and flexibility of our approach through a series of numerical simulations. In these we price European and American put options based upon assets following the CEV process (2.1).

4.1 Price tables

In Tables 1, 2, 3, and 4 we display prices for both European and American puts for values of $\alpha=0, 1/2, 2/3$ and 1, respectively. In these, N is the polynomial order, K is the number

Table 1: Value of European and American puts for the CEV process with $\alpha=0$ for $r=0.05$, $\sigma=0.2$, $S_0=10$, and $T=1/2$.

	European			American		
	$E=9$	$E=10$	$E=11$	$E=9$	$E=10$	$E=11$
$N=2, K=40$	0.1468	0.4423	0.9955	0.1558	0.4673	1.0733
$N=2, K=80$	0.1468	0.4424	0.9955	0.1524	0.4650	1.0757
$N=2, K=160$	0.1468	0.4424	0.9955	0.1515	0.4642	1.0752
$N=2, K=320$	0.1468	0.4424	0.9955	0.1513	0.4640	1.0752
$N=3, K=40$	0.1468	0.4423	0.9955	0.1513	0.4640	1.0750
$N=3, K=80$	0.1468	0.4424	0.9955	0.1513	0.4640	1.0751
$N=3, K=160$	0.1468	0.4424	0.9955	0.1513	0.4639	1.0751
$N=3, K=320$	0.1468	0.4424	0.9955	0.1512	0.4639	1.0751
$N=4, K=40$	0.1468	0.4424	0.9955	0.1516	0.4642	1.0747
$N=4, K=80$	0.1468	0.4424	0.9955	0.1513	0.4640	1.0751
$N=4, K=160$	0.1468	0.4424	0.9955	0.1513	0.4639	1.0751
$N=4, K=320$	0.1468	0.4424	0.9955	0.1512	0.4639	1.0751
Binomial (1000 nodes)	0.1468	0.4423	0.9955	0.1512	0.4638	1.0751
Binomial (5000 nodes)	0.1468	0.4424	0.9955	0.1512	0.4639	1.0751
Exact Solution	0.1468	0.4424	0.9955			

Table 2: Value of European and American puts for the CEV process with $\alpha=1/2$ for $r=0.05$, $\sigma=0.2$, $S_0=10$, and $T=1/2$.

	European			American		
	$E=9$	$E=10$	$E=11$	$E=9$	$E=10$	$E=11$
$N=2, K=40$	0.1360	0.4424	1.0065	0.1434	0.4695	1.0907
$N=2, K=80$	0.1367	0.4421	1.0069	0.1419	0.4657	1.0867
$N=2, K=160$	0.1369	0.4421	1.0070	0.1417	0.4650	1.0860
$N=2, K=320$	0.1369	0.4421	1.0070	0.1416	0.4646	1.0858
$N=3, K=40$	0.1364	0.4416	1.0065	0.1413	0.4643	1.0849
$N=3, K=80$	0.1368	0.4419	1.0068	0.1415	0.4645	1.0854
$N=3, K=160$	0.1369	0.4421	1.0069	0.1416	0.4646	1.0857
$N=3, K=320$	0.1370	0.4421	1.0070	0.1416	0.4646	1.0858
$N=4, K=40$	0.1370	0.4421	1.0071	0.1419	0.4657	1.0844
$N=4, K=80$	0.1370	0.4421	1.0070	0.1416	0.4646	1.0856
$N=4, K=160$	0.1370	0.4421	1.0070	0.1416	0.4647	1.0858
$N=4, K=320$	0.1370	0.4421	1.0070	0.1416	0.4646	1.0858
Binomial (1000 nodes)	0.1370	0.4419	1.0070	0.1416	0.4646	1.0857
Binomial (5000 nodes)	0.1370	0.4421	1.0071	0.1416	0.4646	1.0858
Exact Solution	0.1370	0.4421	1.0070			

Table 3: Value of European and American puts for the CEV process with $\alpha=2/3$ for $r=0.05$, $\sigma=0.2$, $S_0=10$, and $T=1/2$.

	European			American		
	$E=9$	$E=10$	$E=11$	$E=9$	$E=10$	$E=11$
$N=2, K=40$	0.1322	0.4424	1.0101	0.1410	0.4720	1.0986
$N=2, K=80$	0.1334	0.4421	1.0107	0.1391	0.4666	1.0909
$N=2, K=160$	0.1337	0.4420	1.0109	0.1386	0.4654	1.0898
$N=2, K=320$	0.1338	0.4420	1.0110	0.1385	0.4649	1.0887
$N=3, K=40$	0.1329	0.4417	1.0105	0.1381	0.4621	1.0885
$N=3, K=80$	0.1335	0.4419	1.0109	0.1384	0.4637	1.0893
$N=3, K=160$	0.1337	0.4420	1.0110	0.1386	0.4648	1.0894
$N=3, K=320$	0.1338	0.4420	1.0110	0.1385	0.4649	1.0894
$N=4, K=40$	0.1340	0.4420	1.0111	0.1398	0.4672	1.0877
$N=4, K=80$	0.1338	0.4420	1.0110	0.1390	0.4647	1.0893
$N=4, K=160$	0.1338	0.4420	1.0110	0.1386	0.4649	1.0895
$N=4, K=320$	0.1338	0.4420	1.0110	0.1385	0.4649	1.0894
Binomial (1000 nodes)	0.1339	0.4419	1.0110	0.1385	0.4649	1.0894
Binomial (5000 nodes)	0.1338	0.4420	1.0110	0.1385	0.4649	1.0894
Exact Solution	0.1338	0.4420	1.0110			

Table 4: Value of European and American puts for the CEV process with $\alpha=1$ for $r=0.05$, $\sigma=0.2$, $S_0=10$, and $T=1/2$.

	European			American		
	$E=9$	$E=10$	$E=11$	$E=9$	$E=10$	$E=11$
$N=2, K=40$	0.1159	0.4503	1.0108	0.1232	0.4899	1.1186
$N=2, K=80$	0.1266	0.4413	1.0207	0.1352	0.4689	1.1009
$N=2, K=160$	0.1274	0.4420	1.0189	0.1329	0.4667	1.0979
$N=2, K=320$	0.1276	0.4420	1.0191	0.1325	0.4659	1.0971
$N=3, K=40$	0.1250	0.4401	1.0186	0.1301	0.4649	1.0958
$N=3, K=80$	0.1270	0.4415	1.0190	0.1315	0.4654	1.0965
$N=3, K=160$	0.1275	0.4419	1.0191	0.1321	0.4655	1.0968
$N=3, K=320$	0.1276	0.4419	1.0191	0.1324	0.4656	1.0969
$N=4, K=40$	0.1280	0.4419	1.0192	0.1371	0.4729	1.0952
$N=4, K=80$	0.1276	0.4420	1.0191	0.1333	0.4674	1.0975
$N=4, K=160$	0.1276	0.4420	1.0191	0.1326	0.4659	1.0972
$N=4, K=320$	0.1276	0.4420	1.0191	0.1324	0.4656	1.0970
Binomial (1000 nodes)	0.1277	0.4418	1.0191	0.1324	0.4655	1.0970
Binomial (5000 nodes)	0.1276	0.4419	1.0190	0.1324	0.4655	1.0970
Exact Solution	0.1276	0.4420	1.0191			

of elements used, and E is the strike price. Simulations were done on the stock price space $\{0 < S < S_{\max} = 20\}$, and the parameter values $r=0.05$, $\sigma=0.2$, $S_0=10$, and $T=1/2$ were selected. In these we see the rather rapid convergence of our method to the exact solution in the case of European options. For the American derivatives, we resort to highly

resolved binomial simulations [17] and, while we note convergence, it is somewhat less striking than the European case. The choice of parameters was taken from Wong and Zhao [22] where tables are presented for $\alpha=0$ and $\alpha=2/3$, on strike prices of 90, 100, and 110. The grid has been rescaled in our results by a factor of $1/10$, and the cases $\alpha=1/2, 1$ have been added.

4.2 Rates of convergence

Returning to our results from the previous section, we now make our observations regarding the rate of convergence more precise. Beginning with the $\alpha=0$ CEV model, we display convergence results in Figs. 1 and 2 for DG schemes of orders $N=2$ and $N=4$, respectively. These show convergence of our numerical simulation to the exact solution in the case of European options and to a highly resolved binomial simulation for the American version [17]. In Table 5 we report convergence rates, fit by least squares to the relation $e=CK^p$, for both European and American options, in the cases of DG methods of polynomial orders $N=2,4$. For the European cases, our results exceed the predicted rate of $p=-(N+1)$ for N even (see Theorem 7.3 of [15] for the *constant-coefficient* heat equation). However, for the American versions we find rates of convergence in the vicinity of $p=-1.5$. While, on the surface, this seems rather disappointing, we recall that functions of a one-dimensional variable with one (but not two) continuous derivatives, such as the solutions of American pricing problems, can only be approximated by polynomials to order $-3/2$ (see, e.g., [7, p. 72]).

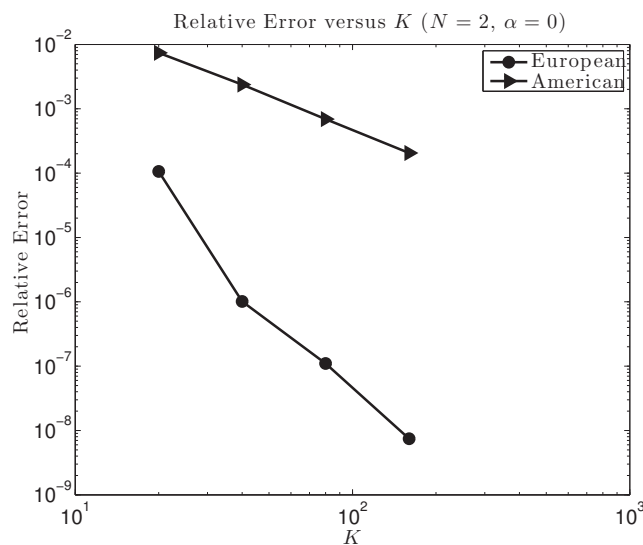


Figure 1: Relative error versus the number of elements, K , in Discontinuous Galerkin (polynomial order $N=2$) simulations of the CEV model ($\alpha=0$).

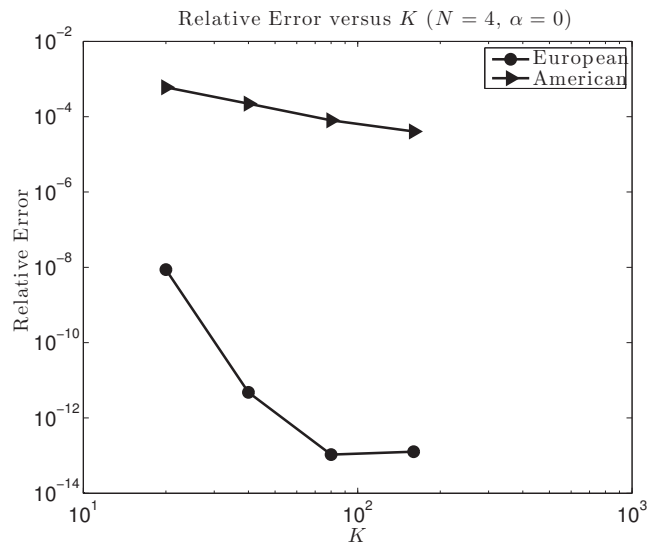


Figure 2: Relative error versus the number of elements, K , in Discontinuous Galerkin (polynomial order $N=4$) simulations of the CEV model ($\alpha=0$).

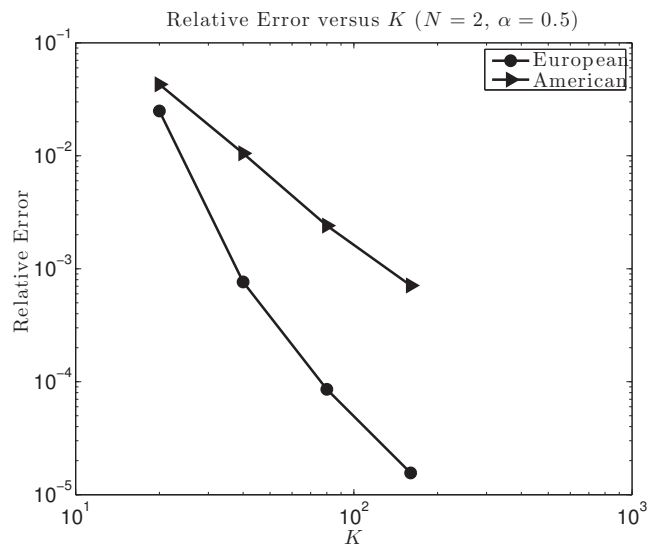


Figure 3: Relative error versus the number of elements, K , in Discontinuous Galerkin (polynomial order $N=2$) simulations of the CEV model ($\alpha=1/2$).

We repeat this experiment in the CEV models with $\alpha = 1/2$ (see Figs. 3 & 4), $\alpha = 2/3$ (see Figs. 5 & 6), and $\alpha = 1$ (see Figs. 7 & 8). In Table 5 we summarize the rates of convergence we measured for each of these α values for $N=2,4$ and European and American options. In all of these, for the European case we see rates of convergence

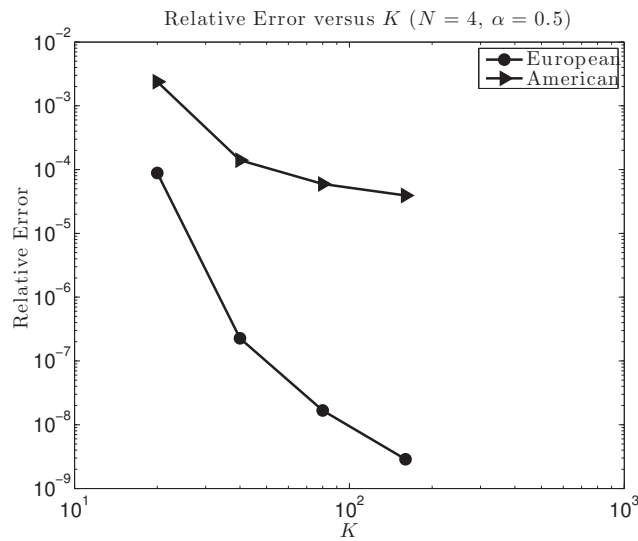


Figure 4: Relative error versus the number of elements, K , in Discontinuous Galerkin (polynomial order $N=4$) simulations of the CEV model ($\alpha=1/2$).

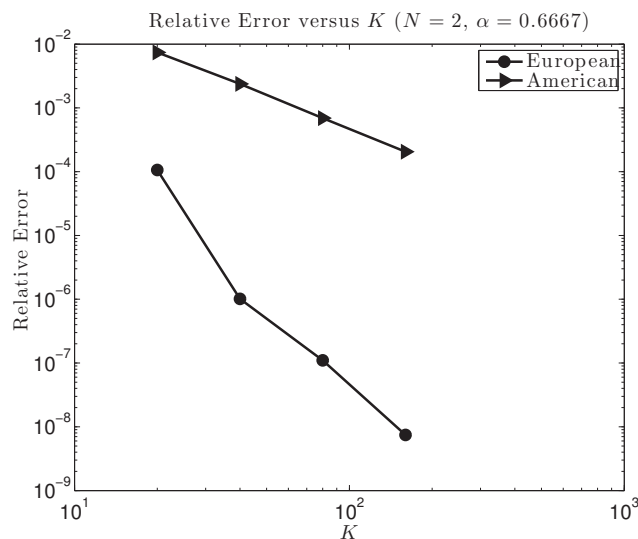


Figure 5: Relative error versus the number of elements, K , in Discontinuous Galerkin (polynomial order $N=2$) simulations of the CEV model ($\alpha=2/3$).

which meet the predicted rate of $p = -(N+1)$ [15]. By contrast, in the American setting, the rate rarely exceeds order two, once again due to the lack of smoothness in the solution.

We close by noting that, while the results above regard the solution as the spot price ($V(10,0)$ in this case) at the initial time, they did not change significantly when our measure of convergence was changed to the supremum (L^∞) norm of the difference of the

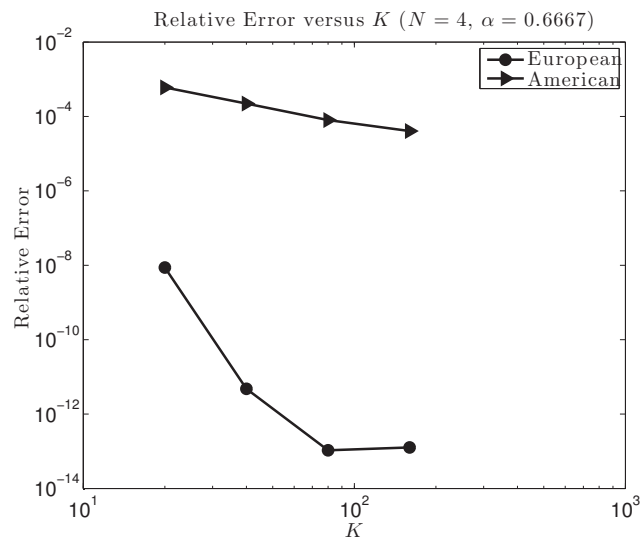


Figure 6: Relative error versus the number of elements, K , in Discontinuous Galerkin (polynomial order $N=4$) simulations of the CEV model ($\alpha=2/3$).

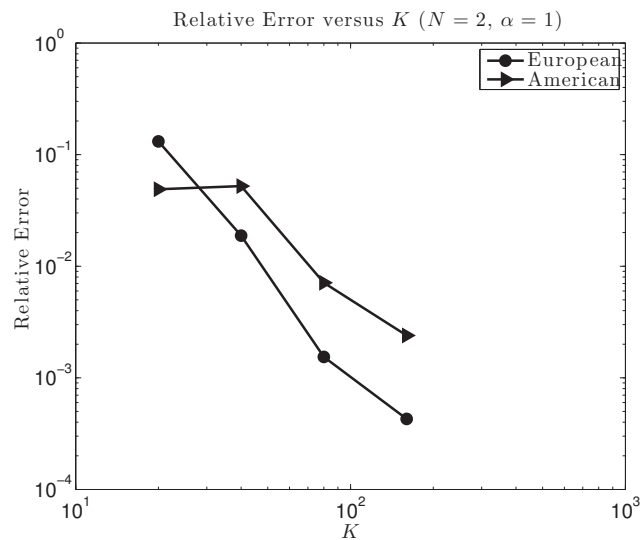


Figure 7: Relative error versus the number of elements, K , in Discontinuous Galerkin (polynomial order $N=2$) simulations of the CEV model ($\alpha=1$).

entire solution at the initial time, $V(S,0)$. Any (minor) degradation from these values we attribute to two factors (see Section 3.1): (i) Our approximation of the inner products in \mathbf{S} , $\tilde{\mathbf{S}}$ and \mathbf{A} , and (ii) The variable coefficient nature of our GBS equation which is quite singular as α decreases (which calls into question not only the error estimates cited earlier, but also the well-posedness theory for (2.7)).

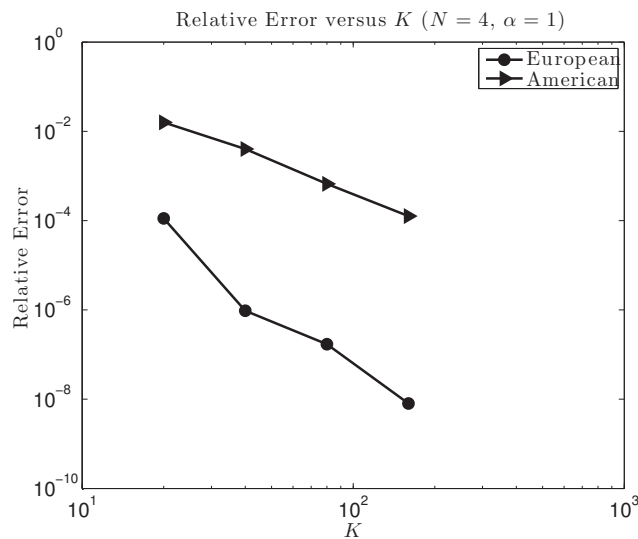


Figure 8: Relative error versus the number of elements, K , in Discontinuous Galerkin (polynomial order $N=4$) simulations of the CEV model ($\alpha=1$).

Table 5: Rates of Convergence for DG scheme applied to European and American puts ($N=2,4$).

α	European				American			
	N	p	N	p	N	p	N	p
0	2	-4.46079	4	-5.36976	2	-1.73034	4	-1.31497
1/2	2	-3.50896	4	-4.85069	2	-1.98726	4	-1.90121
2/3	2	-4.46079	4	-5.36976	2	-1.73034	4	-1.31497
1	2	-2.83961	4	-4.38238	2	-1.59403	4	-2.35263

References

- [1] Y. Achdou and O. Pironneau. Computational methods for option pricing, volume 30 of Frontiers in Applied Mathematics. Society for Industrial and Applied Mathematics (SIAM), Philadelphia, PA, 2005.
- [2] S. Becker. The constant elasticity of variance model and its implications for option pricing. *J. Finance*, 35:661–673, 1980.
- [3] R. Burden and J. D. Faires. Numerical analysis. Brooks/Cole Publishing Co., Pacific Grove, CA, sixth edition, 1997.
- [4] M. J. Brennan and E. S. Schwartz. The valuation of American put options. *Journal of Finance*, 32:449–462, 1977.
- [5] R. Cont, N. Lantos, and O. Pironneau. A reduced basis for option pricing. *SIAM J. Financial Math.*, 2:287–316, 2011.
- [6] J. Cox. The constant elasticity of variance option pricing model. *J. Portfolio Management*, 22:15–17, 1996.
- [7] M. O. Deville, P. F. Fischer, and E. H. Mund. High-order methods for incompressible fluid flow, volume 9 of Cambridge Monographs on Applied and Computational

Mathematics. Cambridge University Press, Cambridge, 2002.

- [8] D. Emanuel and J. MacBeth. Further results on the constant elasticity of variance call option pricing model. *J. Financial and Quantitative Anal.*, 17:533–554, 1982.
- [9] G. Foufas and M. Larson. Valuing Asian options using the finite element method and duality techniques. *Journal of Computational and Applied Mathematics*, 222(1):377–427, 2008.
- [10] P. Glasserman. Monte Carlo methods in financial engineering, volume 53 of *Applications of Mathematics (New York)*. Springer-Verlag, New York, 2004. *Stochastic Modelling and Applied Probability*.
- [11] D. J. Higham. An introduction to financial option valuation. Cambridge University Press, Cambridge, 2004.
- [12] Y. L. Hsu, T. I. Lin, and C. F. Lee. Constant elasticity of variance (CEV) option pricing model: integration and detailed derivation. *Math. Comput. Simulation*, 79(1):60–71, 2008.
- [13] J. Hozman. Discontinuous Galerkin method for the numerical solution of option pricing. In *APLIMAT 2012 (11th International Conference)*, Slovak University of Technology in Bratislava, 2012.
- [14] J. Hull. *Options, Futures, and Other Derivatives*. Prentice Hall, 2012.
- [15] J. S. Hesthaven and T. Warburton. Nodal discontinuous Galerkin methods, volume 54 of *Texts in Applied Mathematics*. Springer, New York, 2008. Algorithms, analysis, and applications.
- [16] C. Knessl and M. Xu. On a free boundary problem for an American put option under the CEV process. *Appl. Math. Lett.*, 24(7):1191–1198, 2011.
- [17] R. Lu and Y.-H. Hsu. Valuation of standard options under the constant elasticity of variance model. *International Journal of Business and Economics*, 4(2):157–165, 2005.
- [18] C. F. Lo, H. M. Tang, K. C. Ku, and C. H. Hui. Valuing time-dependent CEV barrier options. *J. Appl. Math. Decis. Sci.*, pages Art. ID 359623, 17, 2009.
- [19] P. E. J. Vos, S. J. Sherwin, and R. M. Kirby. From h to p efficiently: implementing finite and spectral/ hp element methods to achieve optimal performance for low- and high-order discretisations. *J. Comput. Phys.*, 229(13):5161–5181, 2010.
- [20] P. Wilmott, S. Howison, and J. Dewynne. *The mathematics of financial derivatives*. Cambridge University Press, Cambridge, 1995.
- [21] M. Willyard. *Adaptive Spectral Element Methods To Price American Options*. PhD thesis, Florida State University, 2011.
- [22] H. Y. Wong and J. Zhao. An artificial boundary method for American option pricing under the CEV model. *SIAM J. Numer. Anal.*, 46(4):2183–2209, 2008.
- [23] S. P. Zhu. An exact and explicit solution for the valuation of American put options. *Quantitative Finance*, 6(3):229–242, 2006.